Final Draft
of the original manuscript:

Yan, W.; Rudolph, T.; Noechel, U.; Gould, O.; Behl, M.; Kratz, K.; Lendlein, A.:

Reversible Actuation of Thermoplastic Multiblock Copolymers with Overlapping Thermal Transitions of Crystalline and Glassy Domains.

In: Macromolecules. Vol. 51 (2018) 12, 4624 - 4632.
First published online by ACS: 12.06.2018

https://dx.doi.org/10.1021/acs.macromol.8b00322

Reversible Actuation of Thermoplastic Multiblock Copolymers with Overlapping Thermal Transitions of Crystalline and Glassy Domains

Wan Yan,[1, 2] *Tobias Rudolph*,[1] *Ulrich Noechel,*[1] *Oliver Gould,*[1] *Marc Behl,*[1,3] *Karl Kratz,*[1] *Andreas Lendlein*[*1, 2, 3]

[1] Institute of Biomaterial Science and Berlin-Brandenburg Center for Regenerative Therapies, Helmholtz Zentrum Geesthacht, Kantstr. 55, 14513 Teltow, Germany

[2] Institute of Chemistry, University of Potsdam, 14476 Potsdam, Germany

[3] Tianjin University–Helmholtz-Zentrum Geesthacht, Joint Laboratory for Biomaterials and Regenerative Medicine, Kantstr. 55, 14513 Teltow, Germany

[*]Email: andreas.lendlein@hzg.de

Fax: +49-(0)3328−352 564 452

ABSTRACT

Polymeric materials possessing specific features like programmability, high deformability, and easy processability are highly desirable for creating modern actuating systems. In this study, thermoplastic shape-memory polymer actuators obtained by combining crystallizable poly(ε-caprolactone) (PCL) and poly(3S-isobutylmorpholin-2,5- dione) (PIBMD) segments in multiblock copolymers are described. We designed these materials according to our hypothesis that the confinement of glassy PIBMD domains present at the upper actuation temperature contribute to the stability of the actuator skeleton, especially at large programming strains. The copolymers have a phase-segregated morphology, indicated by the well-separated melting and glass transition temperatures for PIBMD and PCL, but possess a partially overlapping T_m of PCL and T_g of PIBMD in the temperature interval from 40 to 60 °C. Crystalline PIBMD hard domains act as strong physical netpoints in the PIBMD−PCL bulk material enabling high deformability (up to 2000%) and good elastic recoverability (up to 80% at 50 °C above $T_{m,PCL}$). In the programmed thermoplastic actuators a high content of crystallizable PCL actuation domains ensures pronounced thermoreversible shape changes upon repetitive cooling and heating. The programmed actuator skeleton, composed of PCL crystals present at the upper actuation temperature T_{high} and the remaining glassy PIBMD domains, enabled oriented crystallization upon cooling. The actuation performance of PIBMD-PCL could be tailored by balancing the interplay between actuation and skeleton, but also by varying the quantity of crystalline PIBMD hard domains via the copolymer composition, the applied programming strain, and the choice of T_{high}. The actuator with 17 mol% PIBMD showed the highest reversible elongation of 11.4% when programmed to a strain of 900% at 50 °C. It is anticipated that the presented thermoplastic actuator materials can be applied as modern compression textiles.

■ INTRODUCTION

Actuating materials, which are capable of reversibly changing their shape in response to various environmental stimuli, have raised significance as actuators for biomimetic robots, artificial muscles and molecular machines.[1-4] Among the large number of candidate materials for stimuli-driven soft actuators, shape-memory polymers (SMPs) are desirable for their ability to undergo predesignated shape changes and reprogrammability.[5,6] In this context, free-standing reversible motions have been reported for layered or laminated composite structures utilizing a one-way polymer material[5−7] or liquid-crystalline networks[8] and pure semicrystalline copolymer systems with covalent[9−12] or physical netpoints.[13−16] The temperature-responsive actuations in bidirectional reversible SMP systems based on semi-crystalline polymers originate from the melt-induced contraction (MIC) and crystallization-induced elongation (CIE) of actuation domains. Skeleton forming domains composed of orientated crystallizable domains guide shape changes along predesignated routes allowing access to reversible actuation during heating and cooling cycles.[10] The actuation performance of SMPs is highly sensitive to the chemical composition, the morphology, and the degree of orientation of the different functional domains. Therefore, each parameter in an actuator material needs to be balanced according to the environment. Current examples of such tailor-made networks mostly consist of chemically crosslinked networks, which limit their processability and recycling.[10,17,18] On the other hand, using physical netpoints to introduce stability to the material might overcome some of these drawbacks. The possible way of introducing physical netpoints into thermoplastic materials is incorporating crystallizable domains with a high melting temperature.

Currently, SMP-based actuators rely on covalently crosslinked polymer networks.[10, 17-19] For example, networks composed of poly(ω-pentadecalactone) and poly(ε-caprolactone) (PCL),

programmed to only 40% strain, exhibited a reversible elongation of around 20%.[10] Using stable physical crosslinks to replace covalent crosslinks gives thermoplastic actuators clear advantages in reprocessability. Different concepts have been reported to achieve free-standing reversible actuations in thermoplastic shape-memory polymers. Thermoplastics based on copolymers with hard and soft segments can be achieved by polycondensation reactions.[13-15] A freestanding thermoreversible shape change of up to $\Delta\varepsilon$ = 17% has been reported for a commercial poly(ester urethane) composed of poly(1,4-butylene adipate) (PBA) soft domains and 4,4-methylenediphenyl diisocyanate based (chain extended by 1,4-butanediol) hard domains after a tensile deformation up to 1000% and subsequent unloading were applied at 60 °C.[14] During elongation the strain-induced formation of hightemperature stable α crystals of PBA occurs, which function as skeleton domains, while low melting PBA crystals are responsible for expansion and contraction of the actuator. A reversible actuation has been described for thermoplastic ethylene/-1-octene diblock copolymer actuator exhibiting a broad melting transition.[15] Here, domains with longer crystalline ethylene sequence length and respective higher melting temperatures were utilized as skeleton, while domains with shorter ethylene sequence length undergo melting induced contraction (MIC) and oriented crystallization induced elongation (CIE) during cyclic heating and cooling. A reversible two-way shape-memory effect (without external load) was obtained in a commercial poly[ethylene-*co*- (methacrylic acid)] ionomer having a broad melting transition in the range of 56−100 °C, well above the copolymers' order-to-disorder transition of 48 °C.[16] It has been demonstrated for this ionomer system that the reversible shape changes are related to MIC and CIE and not to the order-to-disorder transition as described for other ionomers, e.g., Nafion.[20] Here, high melting polyethylene crystals serve as skeleton, while lower melting crystals are responsible for the thermoreversible actuation.

Furthermore, a free-standing reversible shape-memory effect has been reported for a polyurethane synthesized from 1,6- hexamethylene diisocyanate, PCL, and 1,4-butanediol as chain extender.[13] In this system, the molecular flipping of some PU hard domains in the presence around the PCL soft segments on heating and in the direction of actuation forms the required skeleton, while the reversible elongation around 8% is caused by melting and oriented crystallization of the PCL actuation domains. The reduced actuation capability of thermoplastic SMP-based actuators compared to thermosets obtained by chemical cross-links results from the deformation and subsequent rearrangement and partial destruction of the physical netpoints during programming and thus a less pronounced MIC upon heating. Caused by the reorganization of the physical netpoints a lower degree of orientation of the polymer chains is obtained, which is less effective at guiding the crystallization of actuation domains along the direction of shape change.

Conceptually, the following important parameters need to be considered for polymer networks in order to perform a reversible shape-memory effect, which should help to identify or design a suitable thermoplast. Materials should: (i) form strong physical netpoints (hard domains) to support the overall stability, which could be realized by highly crystalline building blocks or by intramolecular interactions in crystallizable segments with a high melting temperature; (ii) contain a large amount of crystallizable domains with a high actuation performance; (iii) include domains forming a skeleton stabilizing the actuation geometry and guiding the crystallization of the actuation domains; and (iv) have at least one domain with a low glass transition temperature (at least below 0 °C) to enable mobility and flexibility of the system.

A suitable system would be a phase-separated (multiblock) copolymer, in which the individual building blocks combine the required functions into one material. One segment could always integrate/merge two features at the same time, yielding a polymer capable of forming hard domains

in the thermoplastics. From this point of view depsipeptide-based multiblock copolymers with polyester segments are interesting candidates for thermoplastic SMP actuators, e.g., multiblock copolymers comprising crystallizable poly(3S-*iso*-butylmorpholin-2,5-dione) and poly(ε-caprolactone), named PIBMD−PCL, which are linked via urethane bonds.[21] PIBMD, which is a synthetic polydepsipeptide, has a high glass transition temperature ($T_{g,PIBMD}$ ~ 50 °C) and forms crystals with a high melting transition ($T_{m,PIBMD}$ ~ 138 °C) due to the existence of stable hydrogen bonds, similar to proteins.[22] These PIBMD hard domains can therefore act as physical netpoints and improve the overall stability of composite materials enabling retention of the original shape.[23,24] Additionally, the $T_{g,PIBMD}$ is located in the actuation temperature range of PCL domains (~50 °C), which synergistically improves the dual-shape performance in PIBMD−PCL.

We therefore targeted an actuator material based on a linear thermoplastic PIBMD-PCL, exhibiting high deformability, reprocessability and excellent reversible bidirectional actuation performance. Our concept for achieving free-standing reversible actuations in thermoplastic PIBMD−PCL is based on crystalline PIBMD hard domains providing the overall material stability, a large content of PCL actuation domains for achieving pronounced thermoreversible shape changes, and a skeleton built from high melting PCL crystals guiding the oriented crystallization. We further hypothesize that glassy PIBMD domains present at the high actuation temperature T_{high} can additionally contribute to the stability of the skeleton, especially when large strains are applied. For tailoring the actuation performance in PIBMD−PCL the interplay between actuation and skeleton plus crystalline PIBMD hard domains was adjusted by variation of the copolymer composition, the applied programming strain, and T_{high}. A set of PIBMD-PCL with different ratios of these two building blocks were synthesized by polycondensation. Within this study, a series of PIBMDX-PCLY multiblock copolymers (MBCs) with PIBMD contents varying from 38 to 6 mol%

were synthesized to find an optimal composition and to study the influence of the glassy PIBMD fraction on the actuation capability.

The combination of thermal and mechanical testing, FTIR, and X-ray scattering experiments was used to elucidate the material properties of the thermoplastic films giving a detailed insight into the function of crystalline and glassy PIBMD domains. The actuation performance of the prepared PIBMD− PCLs was explored by cyclic uniaxial thermomechanical experiments.

■ EXPERIMENTAL SECTION

Sample preparation. PIBMD*X*-PCL*Y* MBCs were synthesized from different weight ratios of poly(ε-caprolactone)-diol (M_n = 2,700 g mol^{-1}; Solvay Chemicals) and poly(3*S*-*iso*-butyl-morpholin-2,5-dione)-diol[25] (M_n = 4,000 g mol^{-1}), which were reacted with trimethyl hexamethylene diisocyanate (TMDI) as a junction unit using dibutyltin dilaurate as a catalyst as described in ref.[21]. Homopolymers and copolymers were denoted as PIBMD*X*-PCL*Y*, where *X* and *Y* indicate the molar fraction (mol%) of the respective diol in the feed solution. 2.28g of PIBMD*X*-PCL*Y* was dissolved in chloroform overnight at ambient temperature, and later the solution was poured into a glass Petri dish (diameter = 80 mm) to evaporate the chloroform over 5 days. The resulting film thickness was determined to be 250±30 µm. Then the test specimens were cut with a type DIN EN ISO 527-2/1BB punch (total length = 30 mm, width in the middle of the specimen = 2 mm) for further investigation.

Differential scanning calorimetry (DSC). DSC experiments were conducted on a Netzsch DSC 204 Phoenix (Selb, Germany) at heating and cooling rates of 10 K·min^{-1} in pierced aluminum pans. For determining the thermal properties of the copolymers, the materials were investigated in the temperature range from -100 to 200 °C. The crystallinity of PCL domains ($x_{c,PCL}$) was calculated according to the equation (1):

$$x_c = \frac{\Delta H_m}{\Delta H_m^{100}} \times \frac{1}{W_{PCL}} \times 100 \quad (1)$$

Here, ΔH_m is the melting enthalpy, representing the area of the melting peak. ΔH_m^{100} is the specific melting enthalpy for a 100% crystalline PCL, which was 135 J·g^{-1} [26], and W_{PCL} is the weight percentage (wt%) of PCL domains in PIBMD*X*-PCL*Y* MBCs. For the measurement of programmed specimens, samples were heated to 75 °C for 10 min before they were cooled to 0 °C and heated to 200 °C.

Fourier transform infrared spectroscopy (FTIR). FTIR measurements (Bruker-Optics, α-Alpha-P and Shimadzu, FTIR-8400S) were performed using thin solution-casted films of PIBMD*X*-PCL*Y* samples placed on the ATR unit. Measurements were performed in absorbance in the range from 600 to 4000 cm^{-1} with a resolution of 2 cm^{-1}.

Mechanical tests. All mechanical tests were performed with a thermomechanical tensile tester (Zwick Z1.0, Ulm, Germany) equipped with a thermo-chamber and temperature controller (Eurotherm Regler, Limburg, Germany). Because of the size of the thermochamber, the maximum distance between the two clamps was 300 mm; the clamping distances of the test specimens were adapted to a distance of 15 mm for experiments reaching elongations between 200, 400, and 900%, while a clamping distance of 10 mm was applied in experiments with elongations ranging from 1200 to 1800%. Elongations at break of the samples were tested by stretching the sample at different testing temperatures with a strain rate of 10 mm·min^{-1} until breakage occurred. Loading/unloading tensile tests were performed by loading to a training strain at a programming temperature with a strain rate of 10 mm·min^{-1} and unloading with the rate of 0.06 N min^{-1}. This procedure was performed for 3 cycles, followed by the tensile test with a strain rate of 10 mm·min^{-1} until break. The actuation performance of the samples was characterized by programming and

reversibility modules consisting of three repetitive cycles. In a programming module, test specimens were first heated to 75 °C without applying any stress and kept at these conditions for 10 min to erase any thermal history. Then the temperature was reduced to a programming temperature (T_{prog}), and the specimens were deformed to a desired strain at a strain rate of 10 mm min^{-1}. Subsequently, the deformed specimens were kept at T_{prog} for 5 min to allow relaxation and the temporary shapes were fixed by cooling to 0 °C. The reversibility module consisted of heating the sample to a high actuation temperature (T_{high}) followed by a waiting period of 10 min and subsequential cooling to a low actuation temperature (T_{low}) and waiting for another 20 min. Heating and cooling rates were 2 and 5 °C·min^{-1}. A photo series illustrates actuator programming of PIBMD17-PCL79 with ε_{prog} = 900% (Supporting Information, Figure S13).

The deformation fixation efficiency Q_{eff} was calculated as ratio between the elongation of the sample at T_{high} and the programmed elongation ε_{prog} according to eq 2.

$$Q_{eff} = \frac{\varepsilon(T_{high})}{\varepsilon_{prog}} * 100 \quad (2)$$

The reversible elongation (ε'_{rev}) was calculated according to following equation (3):

$$\varepsilon'_{rev} = \frac{l_B - l_A}{l_A} * 100 = \frac{\varepsilon_B - \varepsilon_A}{(\varepsilon_A + 100)} * 100 \quad (3)$$

Here, l_A and l_B are the length of the test specimen at T_{high} and T_{low}, and ε_A and ε_B are the strain of the test specimen at T_{high} and T_{low}, respectively.

Wide-Angle X-ray Scattering (WAXS). WAXS measurements were performed on a D8 Discover with a two-dimensional detector from Bruker AXS (Karlsruhe, Germany) at various temperatures ranging from 0 to 75 °C. WAXS patterns were recorded with an exposure time of 120 s per

scattering pattern. The relationship of the integrated areas of crystalline and amorphous regions determines the overall degree of crystallinity (*DOC*) according to equation (4):

$$DOC = \frac{A_{cryst}}{A_{cryst} + A_{amorph}} \times 100 \quad (4)$$

where A_{amorph} is the area under amorphous halo and A_{cryst} the area of the crystalline peaks.

■ RESULTS AND DISCUSSION

Synthesis and Characterization of Multiblock copolymers

For the synthesis of multiblock copolymers (MBCs), different molar ratios of the building blocks, poly(ε- caprolactone) (PCL) and poly(3S-isobutylmorpholin-2,5- dione) (PIBMD), were used for the polycondensation reaction with trimethyl hexamethylene diisocyanate (TMDI) as a junction unit.[21] Homopolymers (PIBMD*00*-PCL*96* and PIBMD*96*-PCL*00*) and copolymers (PIBMD*38*-PCL*60,* PIBMD*30*-PCL*66,* PIBMD*17*-PCL*79,* and PIBMD*06*-PCL*92)* were obtained and characterized, concerning their physical properties as listed in **Table 1** and **Supporting Information, Table S1**. Numbers in PIBMD*X*-PCL*Y* denote the respective molar fraction (*mol*%) of the polymer in the feed solution, while TMDI is in a similar range of 4 *mol*% for all of the copolymers. The molar mass of all MBCs was kept in a similar range of around 50 000 g mol^{-1}, allowing to correlate all the following findings solely to the composition. According to differential scanning calorimetry (DSC), PCL domains in all copolymers show a $T_{m,PCL}$ around 42±4 °C and the $T_{g,PCL}$ at -57±2 °C (**Supporting Information**, **Figure S1**). While the $T_{m,PIBMD}$ of PIBMD domain was determined to be 138±2 °C, the $T_{g,PIBMD}$ overlaps with the melting peak of PCL in the DSC. In DMTA measurements a $T_{\delta,max}$ ~ 60±5 °C was found for PIBMD38-PCL60 and PIBMD30-PCL66, while for copolymers with higher PCL content no maximum was observed

(**Supporting Information**, **Figure S2**). The PCL crystallinity (x_{PCL}) calculated from DSC thermograms is decreasing as the PIBMD content is increasing in the respective PIBMD*X*-PCL*Y* films from 41±2 wt% to 10±2 wt% from PIBMD*00*-PCL*96* to PIBMD*38*-PCL*60*, respectively (**Table S1**). Well separated T_gs and T_ms indicate their phase separation and the size of separated phases in MBCs are usually limited in the nano-scale.[27,28] Interestingly, DSC data for the copolymers from the first heating ramp (**Figure 1a**, dashed lines), after annealing at 75 °C, indicate that PCL domains in PIBMD*38*-PCL*60* cannot crystallize during cooling from melt with a cooling rate of 5 °C min^{-1}, while for PIBMD*30*-PCL*66*, PIBMD*17*-PCL*79* and PIBMD*06*-PCL*92*, clear PCL melting peaks at 40±2 °C are observed. This observation could be explained by morphological competition between the confinement/restriction from the glassy PIBMD domains and the crystallization of PCL domains. Especially, in PIBMD*38*-PCL*60*, the glassy PIBMD chains restrict the crystallization of PCL domains during cooling.[29] In the other three samples, PCL forms the continuous matrix, where PIBMD domains have less influence on their crystallization behavior. T_m corresponding to the PIBMD is not influenced, and only the intensity is changed by the composition of the copolymers. The reason for the high melting temperature of PIBMD is the formation of strong hydrogen bond interactions between the IBMD repeating units, enabling the formation of thermally stable crystals. Measurements by FTIR applied to the PIBMD*X*-PCL*Y* films (**Supporting Information**, **Figures S3, S4, and S5**) confirm the presence of hydrogen bonds formed between –NH– and –C=O in amide groups within IBMD chain segments. In the region of stretching vibrations of –C=O groups, the bands at 1650 and 1680 cm^{-1} are assigned to the hydrogen-bonded and free –C=O in amide groups.[30-32] The peaks in this region were fitted concerning the area below enabling to determine the interaction in the respective composition (**Figure S4**). The results indicate, by calculating the ratio of the peak areas, that around 55% amide groups in PIBMD domains formed hydrogen bonds within PIBMD*38*-PCL*60*. This value

decreases to around 46%, 44%, and 32% when the PIBMD content is reduced to 30%, 17%, and 6% as listed in **Table 1**. Additionally, the secondary structure of peptides is reflected by the location of amide I bands and the absorptions at 1650 cm^{-1} of bonded amide groups demonstrated its α-helix structures as illustrated in **Figure S4**.[33] Temperature-dependent FTIR measurements also confirm the stability of the hydrogen bonds in the PIBMD domains (**Figure S5**) in the range of 20 to 75 °C. These results illustrate the successful introduction of physical crosslinks by the PIBMD microdomains, whereby the PIBMD crystals supported by hydrogen bonds serving as netpoints are sufficiently stable to withstand a high strain deformation without breakage at elevated temperatures.

In the next step, the postulated influence/contribution of the glassy PIBMD domains on the mechanical properties was investigated in detail to give insights into possible morphological and macromolecular changes. Choosing a deformation temperature of 50 °C, which is close to the $T_{g,PIBMD}$ (far above $T_{g,PCL}$) and above $T_{m,PCL}$, should enable synergies in the interaction of the respective domains under deformation. Stretching amorphous polymer chains leads to an elongation and orientation of remaining crystallites, while glassy domains start to change their position and partially dislocate the domains from the original position at high strains.[34-40] Furthermore, at very high deformation ratios, stretching could induce morphological changes of the PIBMD domain itself, as PIBMD is in the transition range between the glassy state and the semi-crystalline state enabling deformability along the deformation direction and due to interfacial stress transport from PCL phase (**Scheme 1**). This would initiate local restrictions for the amorphous PCL domains, which would be in direct dependence to the composition of the individual blocks. **Scheme 1** depicts a 2D illustration of a postulated translation from the different

domains to simplify some predictions, while in the three-dimensional material it will be even more complex.

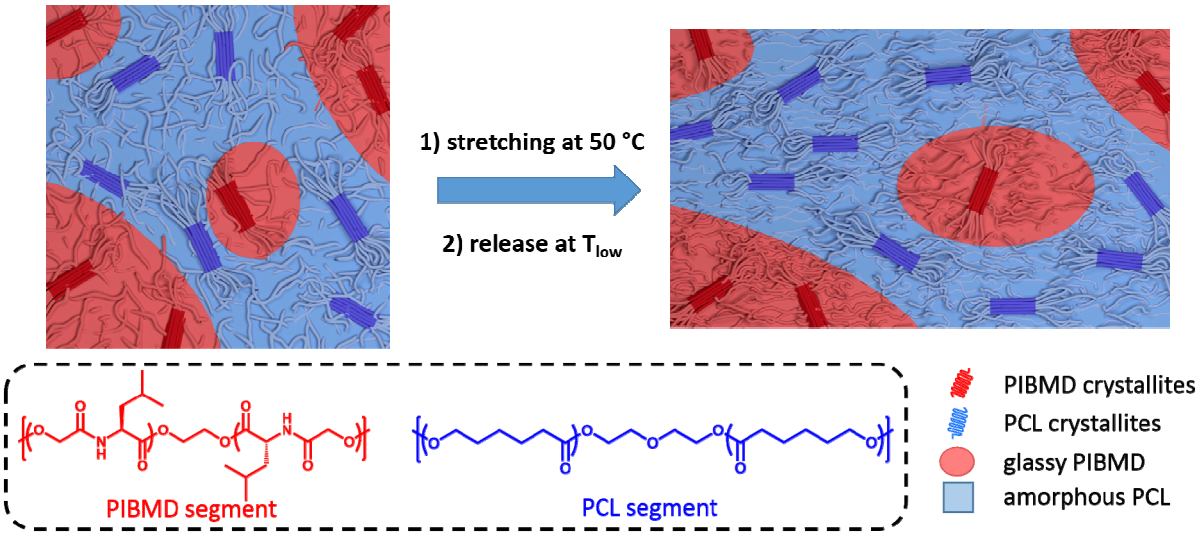

Scheme 1. Chemical structures of PCL and PIBMD segments; homogenous distribution of crystalline and glassy PIBMD segments (red) in a semi-crystalline PCL matrix (blue) before and after stretching at 50 °C enabling morphological changes in the material.

Table 1. Physical properties of PIBMD*X*-PCL*Y* MBC series.

Composition[a]	$T_{m,PCL}$[b] [°C]	$T_{m,PIBMD}$[b] [°C]	DOC_{PIBMD}[c] [%]	$r_{CO,bonded}$[d] [%]	$E_{25°C}$[e] [MPa]	$E_{50°C}$[e] [MPa]	$\varepsilon_{b,50°C}$[f] [%]
PIBMD*00*-PCL*96*	46±2	-	-	-	155±12	-	-
PIBMD*06*-PCL*92*	44±2	-	1.8±0.5	32±5	135±13	3.5±0.5	1900±200
PIBMD*17*-PCL*79*	44±2	138±2	4.6±1.0	46±3	170±5	7.2±0.7	1270±90
PIBMD*30*-PCL*66*	43±2	141±2	14.7±0.8	44±2	245±10	2.6±0.4	1600±580
PIBMD*38*-PCL*60*	42±2	138±2	14.2±2.2	55±1	140±31	17±3	1100±210
PIBMD*96*-PCL*00*	-	167±2	44.6±0.9	63±2	1400±40	129±14	3.5±0.5

[a] named according to the molar ratio.
[b] $T_{m,PIBMD/PCL}$: melting transition temperature of PIBMD/PCL crystals, determined by DSC.
[c] DOC_{PIBMD}: degree of crystallinity of PIBMD domains, calculated from WAXS at 75 °C.
[d] $r_{-CO,bonded}$: ratio of hydrogen bonded –C=O in amide groups, calculated via FTIR measurement at room temperature.
[e] $E_{25°C}$, $E_{50°C,}$ *and* $\varepsilon_{b,50°C}$ represent the elastic modulus at 25 and 50 °C and elongation at break at 50 °C, determined by tensile tests.

Mechanical Properties of Multiblock Copolymers with Different Compositions

The mechanical properties under uniaxial stretching were determined for the set of films as listed in **Table 1**. PIBMD*96*-PCL*00* is very brittle at room temperature with a high Young´s modulus of 1400 MPa, while the Young´s modulus decreased drastically to 129 and 44 MPa at 50 °C and 80 °C when the PIBMD glass transition temperature is exceeded. For PIBMD*X*-PCL*Y* films with more than 60 mol% PCL, the Young´s moduli are mostly dominated by the semi-crystalline PCL matrix, modulating it in the range of 140 to 250 MPa at 25 °C and decreased to 2 to 20 MPa at 50 °C. The elongation at break (ε_b) for all PIBMD*X*-PCL*Y* films were above 1000% at 25 and 50 °C, where the PCL domains are in an amorphous state, indicating highly deformable/stretchable samples (**Table 1**, **Supporting Information Figure S6**). For classical chemically crosslinked polymeric actuator materials, such high deformability is rarely described in the literature as the deformation is restricted by interchain linkage.[10] In physically crosslinked networks deformation leads to a displacement of domains without rupture of bonds but alignment of macromolecules along the stretching direction.[36] This deformability of PIBMD*X*-PCL*Y* films can be further increased using training cycles, which should lead to even higher degrees of alignment of individual polymer chains or domains[39] or can lead to strain-induced crystallization.[14] As an example shown in **Figure 1b**, PIBMD*17*-PCL*79* films are firstly stretched to 1200% at 50 °C and subsequently allowed to relax after releasing the stress. The material is able to recover to ~250% of the original strain as the molten amorphous PCL domains are able to relax, while the glassy/crystalline PIBMD segments stabilize the material. After three training cycles to 1200%, pre-orientation of the polymer chains lead to ultrahigh values of ε_b of around 2000%. Similar effects were found for all compositions (**Supporting Information, Figure S7**), whereby interestingly the materials PIBMD*17*-PCL*79* and PIBMD*38*-PCL*60* are able to relax in between the cycles from high strain

to ~250% upon release of the stretching force, while for PIBMD*06*-PCL*92* and PIBMD*30*-PCL*66* relaxation is reduced, from 1200% to ~800%. A similar trend was found for the deformation fixation efficiency Q_{eff}, which is defined as ratio between elongation of the actuator at T_{high} ($\varepsilon(T_{high})$) and the applied programming elongation ε_{prog} according to eq 2. Therefore, Q_{eff} obtained in actuator programming is different from the shape fixity ratio R_f determined in one-way shape-memory effects by the ratio of the applied deformation strain at T_{high} and the resulting strain at T_{low} after stress is released. It could be demonstrated for covalently cross-linked multiphase copolymer networks that lower deformation fixation efficiencies correlate with a higher reversible actuation performance. An increase of Q_{eff} with increasing amounts of PCL would indicate low possibilities for elongated PCL chains to recover into the coiled state, which at the same time is showing weak abilities of the PIBMD domains to act as strong physical netpoints stabilizing the original shape. As shown in Figure 1c, the lowest Q_{eff} values are obtained for PIBMD17-PCL79 with Q_{eff} around 30% for ε_{prog} = 900% or 1800%, which is remarkable and can only be assumed to correlate with morphological changes (Scheme 1). With respect to our previous findings for covalently cross-linked multiphase copolymer networks with PCL actuation domains,[10,17] where a higher actuation performance was obtained for systems with low Q_{eff} values, a high actuation performance can be expected for PIBMD17-PCL79.

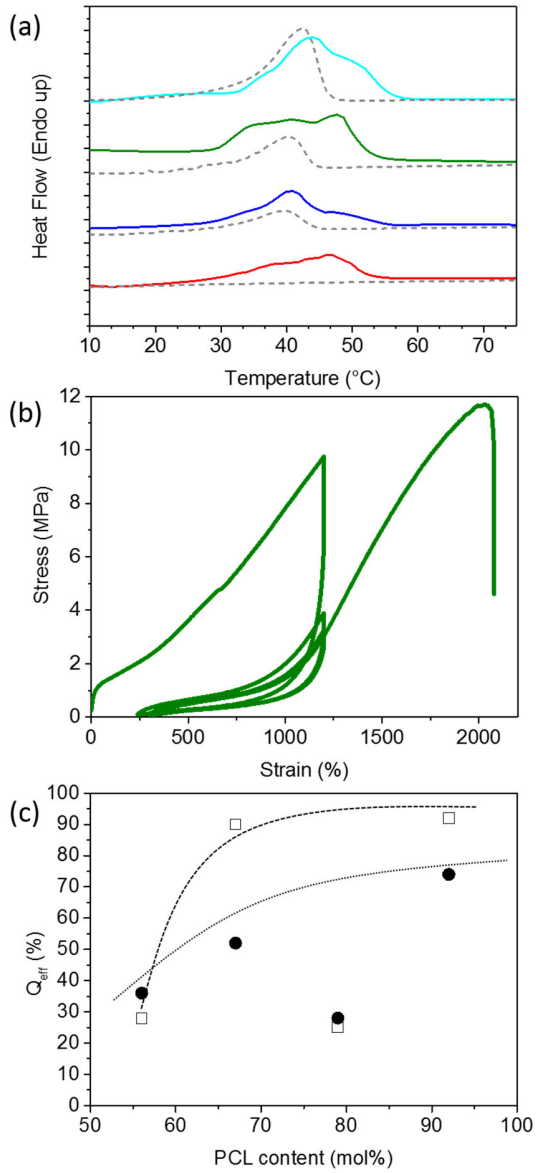

Figure 1: (a) Comparison of DSC thermograms of 1st heating ramp for PIBMD*06*-PCL*92* (cyan), PIBMD*17*-PCL*79* (green), PIBMD*30*-PCL*66* (blue) and PIBMD*38*-PCL*60* (red) after programming to 900% strain and fixing at 0 °C and before programming (dashed line); (b) High deformability enabled for PIBMD*17*-PCL*79* by training cycles after stretching first to 1200% and subsequent release of the stress at 50 °C. (c) Deformation fixation efficiency (Q_{eff}) in dependence to the PCL content and the straining ratio of 900% (filled symbols) and 1800% (empty symbols); lines should guide the eye to the expected trend.

DSC investigations of stretched (and subsequently cooled under stress) samples indicate that for elongations of 900% (or ~1800%; **Figure 1a**) strain-induced crystallization and alignment of the

macromolecules leads to changes in the thermogram in comparison to the pristine samples. For all four compositions the melting peak is broader and indicates the formation of crystals with higher and lower thermal stability (**Figure 1a**) while the x_{PCL} only increased slightly (**Table 2**). The smaller crystals are mostly corresponding to stretching-induced crystal formation and fragmentation upon alignment of polymer chains along the stretching direction. In our case, glassy/crystalline PIBMD domains introduce a stabilizing feature to the material properties as the driving force for relaxation to the original shape is solely attributed to the PCL segments. Observations of large hysteresis is usually correlating to irreversible structural changes in the material, which might indicate that for PIBMD*06*-PCL*92* and PIBMD*30*-PCL*66* the balance between PCL and physical netpoints is not effective leading to plastic unrecoverable deformation.[36]

Table 2. Physical properties of films obtained for PIBMD*X*-PCL*Y* MBC series before and after stretching to 900%.

Composition	Before stretching			After stretching to 900%		
	$T_{m,PCL}$[a] [°C]	$T_{m,PCL,offset}$[a] [°C]	$x_{c,PCL}$[a] [%]	$T_{m,PCL}$[a] [°C]	$T_{m,PCL,offset}$[a] [°C]	$x_{c,PCL}$[a] [%]
PIBMD*06*-PCL*92*	42±2	48±2	32±2	44±2/49±2	59±2	39±2
PIBMD*17*-PCL*79*	40±2	46±2	30±2	41±2/48±2	56±2	33±2
PIBMD*30*-PCL*66*	40±2	46±2	23±2	41±2/47±2	58±2	25±2
PIBMD*38*-PCL*60*	-	-	-	42±2/47±2	56±2	27±2

[a] $T_{m,PCL}$: the melting transition of PCL domains, $T_{m,PCL,offset}$: the offset of PCL melting transition peak, $x_{c,PCL}$: the crystallinity of PCL domains, obtained from the 1st heating curves from DSC measurements.

For additional insights into the morphological changes upon stretching, X-ray scattering measurements of samples stretched to 900% were conducted. All the samples have been stretched followed by subsequent cooling to 0 °C, and release of the force in the thermochamber of the tensile tester before transferred to the measurement. Because of this procedure, stress-free and relaxed samples were investigated. Before and after stretching the average lateral crystal size (l_c)

for PIBMD and PCL was determined and compared to the composition ratio (**Supporting Information, Figure S8**). Here, the apparent crystal size for PIBMD is constant, around 15 nm, independently from the composition before stretching and decreased afterwards to 12.5 nm on average, indicating partial fragmentation of the PIBMD crystals during the deformation step. PCL shows a growth of the respective apparent average size, also depending on the available PCL amount. While the degree of orientation along the stretching direction for PCL is confirmed for increasing amounts of PCL, PIBMD crystals show no preferential orientation after stretching to 900% (**Supporting Information, Figure S9**).

This balance of confinement for PCL influencing the orientation, and the stabilizing influence of PIBMD on the PCL phase allows plastic deformation of the PCL phase, while PIBMD is still in the glassy/crystalline state. This synergy between the two effects should be investigated in the following to study their influence on the reversible bidirectional actuation performance, in which the amount of crosslinks and actuation domains are of importance.

Actuation Capability of Multiblock Copolymers

All the above-mentioned results underline the successful implementation of the design criteria and requirements defined for actuator materials. Based on the mechanism of reversible shape changing, crystallization and the partial melting of oriented crystals in PCL domains enable a thermally controlled actuation capability. The small amount of PCL crystals with higher thermal stability, which can maintain at high actuation temperatures, serve as skeletons to guide the direction of PCL crystallization. If the temperature is not far from the T_g of PIBMD domains, such as 50 °C, orientated PIBMD glassy chains isolated in the PCL domains can also help to keep the orientation of the PCL domains, resulting in oriented crystallization upon cooling.

The actuation performances of different PIBMD*X*-PCL*Y* samples were evaluated by pre-programming the samples to 900% at 50 °C, and setting T_{high} and T_{low} as 50 °C and 5 °C for 3 cycles. Negligible actuation can be observed for programmed PIBMD38-PCL60 specimens. As presented in **Figure 2**, the reversible elongations (ε'_{rev}) for PIBMD30-PCL66 and PIBMD*17*-PCL*79* increases from of 2.0±0.3% to 11.4±1.4% and then decreases to 6.6±0.4% for PIBMD06-PCL92. The compositions of the different MBCs and the crystallite content capable to contribute to the actuation extracted from the DSC thermograms (**Supporting Information, Figure S10**) allow to determine the PCL fraction (*mol*%) correlated to the performance in the temperature range from 10 to 50 °C. This shows a linear increase of the reversible elongation (ε'_{rev}) at a programming strain of 900% in accordance with the actuating content of PCL as expected. Reaching a maximum for PIBMD*17*-PCL*79*, while ε'_{rev} drops for PIBMD*06*-PCL*92,* even so the fraction accessible for actuation is increasing. As expected, PIBMD*17*-PCL*79* exhibiting the lowest deformation fixation ratio Q_{eff} showed the best actuation performance, which is in line with our previous finding for covalently crosslinked actuator materials with PCL actuation domains.[10,17] Therefore, PIBMD17-PCL79 films were chosen to more broadly investigate the influence of varying the testing parameters like programming strain and T_{high}. When programming strains was reduced from 900% to 400% and 200%, the reversible elongation was reduced from 11.4±1.4% to 7.4±1.3% and 6.5±1.0%, as shown in **Figure 2a** (and **Supporting Information, Figures S11, S12, and S14**). This effect can be attributed to the reversible shape change being directly proportional to the overall programming strain. It is clear that a lower degree of orientation is introduced by lower strain during stretching. Further increasing the strain to 1800% by a pre-training, the actuation performance did not improve a lot, since polymer chains were already highly oriented at 900% and instead resulted in the destruction/fragmentation of PIBMD and PCL crystallites. For the other

compositions high straining ratios were tested as well, showing no improvement of the performance (**Figure 2**).

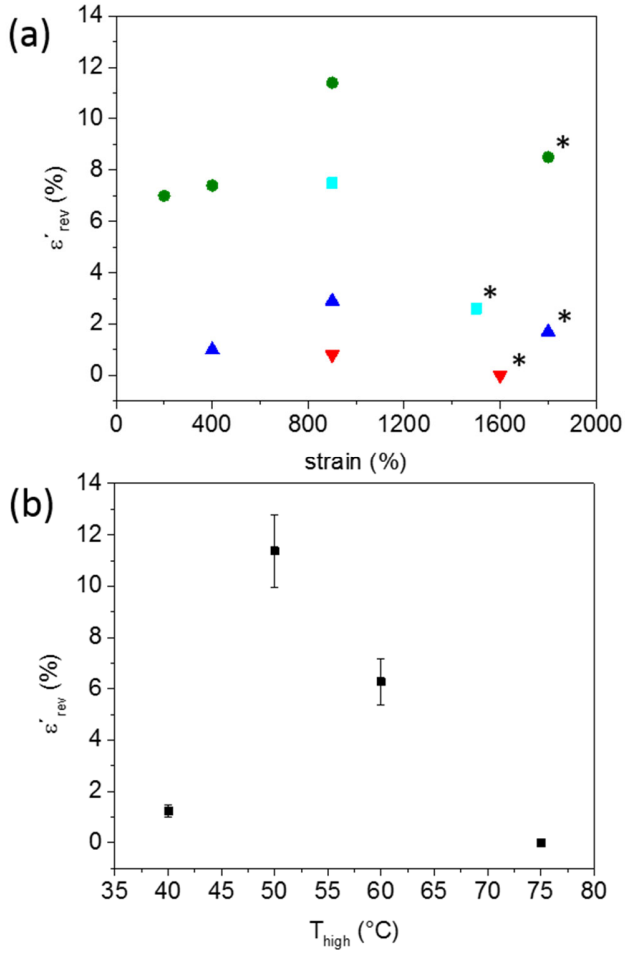

Figure 2. Calculated reversible elongations of (a) PIBMD*17*-PCL*79* (green), PIBMD*06*-PCL*92* (cyan), PIBMD30-PCL66 (blue), and PIBMD38-PCL60 (red) as a function of programming strain when the T_{high} was kept at 50 °C [asterisk indicate that values were obtained after applying three training cycles before programming at the respective strain] and (b) PIBMD*17*-PCL*79* as a function of T_{high} when the programming strain was kept at 900%.

Beside the effect attributed to the programming strain, the variation of T_{high} lowered to 40 °C or increased to 60 °C resulted in a decreased reversible actuation as shown in **Figure 2b** and **Supporting Information, Figure S14**. Changes in the ratios of PCL crystals for actuation and the

skeleton domains reduce the performance, and the stability the T_g of PIBMD is also exceeded. As summarized from WAXS measurement of PIBMD*17*-PCL*79* after programming to 900%, **Figure 3a** indicates that orientated PCL crystals start to melt at 30 °C and are completely molten at 60 °C correlating with the degree of crystallinity (DOC). DOC in PCL crystals upon heating is presented in **Figure 3b**. The PIBMD crystals were not affected in this temperature range (**Supporting Information, Figure S14**). At 40 °C, less than half of the PCL crystals were molten, reducing the amount of actuation domains. At 50 °C, it shows that 90% of the PCL crystals cannot contribute as they are molten, while 10% of them remained to guide the crystallization of PCL during cooling. By increasing T_{high} to 60 °C where all PCL crystals were molten, only some oriented PIBMD glassy chains in the phase boundary can keep the chain alignments within the material, which is much weaker than crystals in PCL domains. The calculation in crystallinity of PCL domains from DSC curves is fully compatible with the results in WAXS. Further increasing to 75 °C, where all PCL crystals are molten and PIBMD chains are transformed into a rubbery state, all internal stress is relaxed and orientation is eliminated. The PIBMD*17*-PCL*79* samples totally recovered to 130±5% after the programming of 900% associated with a sufficient amount of PIBMD crystals. No shape change can be performed after erasing, after which it can be reprogrammed to any other defined temporary shapes.

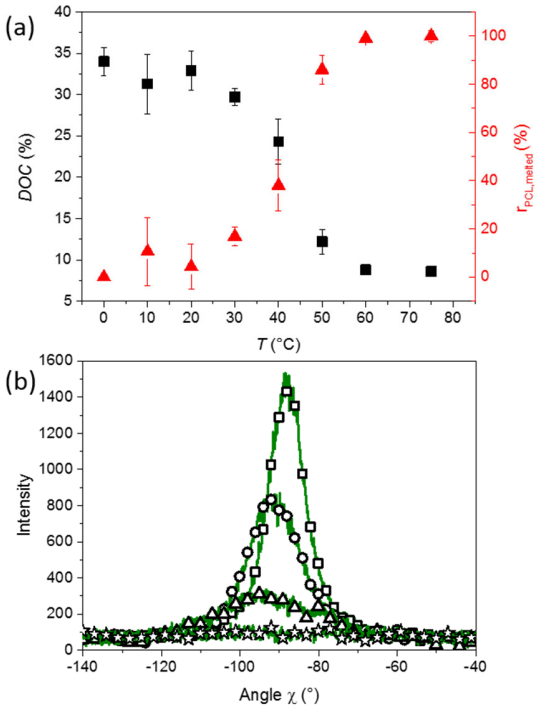

Figure 3. (a) Variation in *DOC* (black square) and ratio of molten PCL crystals (red triangles calculated from WAXS in PIBMD*17*-PCL*79* after programming to 900% as a function of temperature; (b) Azimuthal scan of PCL crystal from WAXS patterns at 0 (squares), 40 (spheres), 50 (triangles), and 60 °C (stars).

■ CONCLUSION

Thermoplastic PIBMD*X*-PCL*Y* MBCs have been successfully utilized to fabricate highly deformable actuating materials enabling to show the influence of PIBMD domains on the actuation capability of PCL. On this example we were able to show materials with high T_m crystals supported by strong hydrogen bonds, forming stable physical networks to remember the original shape of the specimen. Additionally, the influence/contribution of the individual building blocks was shown on the reversible actuation performance and high deformability. For PIBMD*17*-PCL*79* the morphology and the nature of the polymer segments lead to a material, which at 50 °C is amorphous and flexible but, on the other hand, still in the glassy state. This combination benefits shape and macromolecule relaxation at the same time. While for the other compositions (besides PIBMD*17*-PCL*79*) restriction or dilution effects influence the behavior under the thermomechanical treatment. Morphological changes correlating to the physical properties and stress transfer of the building blocks at the respective working temperature enhance the actuation performance and lead to a reversible elongation of up to 11.4% for PIBMD*17*-PCL*79*, which can be classified as good performance in comparison to the actuation efficiency of other pure thermoplastic SMP actuators. Furthermore, this work represents an important step towards the production of reprocessable thermoplastic soft actuators with excellent deformability, a characteristic vital for their application in a variety of fields, e.g. as modern compression textiles.

■ Acknowledgements:

The authors thank Mr. Olaf Lettau for synthesis of PIBMD*X*-PCL*Y*, and Moritz von der Lühe (Friedrich-Schiller University Jena) for temperature dependent FTIR measurements. This work was financially supported by the Helmholtz-Association through programme-oriented funding as

well as through a fellowship for W.Y. by the Helmholtz Graduate School for Macromolecular Bioscience (VH-GS-503) and the Tianjin University-Helmholtz-Zentrum Geesthacht, Joint Laboratory for Biomaterials and Regenerative Medicine, which is financed by the German Federal Ministry of Education and Research (BMBF, Grant No. 0315496) and the Chinese Ministry of Science and Technology (MOST, 2008DFA51170). W.Y. acknowledges financial support by the German Federal Ministry for Education and Research (MIE project, Grant 031A095).

■ Associated Content:

Supporting Information

The Supporting Information is available free of charge on the ACS Publications website at DOI: 10.1021/acs.macromol.8b00322.

Characterization methods, DMTA measurements, tensile test, FTIR results, actuation performance test and the list of physical properties of PIBMD*X*-PCL*Y* samples.

■ REFERENCES

1. Majidi, C. Soft robotics: a perspective—current trends and prospects for the future. *Soft Robotics* **2014,** 1 (1), 5-11.
2. Asaka, K.; Okuzaki, H., *Soft Actuators: Materials, Modeling, Applications, and Future Perspectives*. Springer: 2014.
3. Choi, H. R.; Jung, K.; Ryew, S.; Nam, J.-D.; Jeon, J.; Koo, J. C.; Tanie, K. Biomimetic soft actuator: design, modeling, control, and applications. *IEEE/ASME transactions on mechatronics* **2005,** 10 (5), 581-593.
4. Yeo, J. C.; Yap, H. K.; Xi, W.; Wang, Z.; Yeow, C. H.; Lim, C. T. Flexible and Stretchable Strain Sensing Actuator for Wearable Soft Robotic Applications. *Adv. Mater. Technol.* **2016,** 1 (3), 1600018.
5. Chen, S.; Hu, J.; Zhuo, H.; Zhu, Y. Two-way shape memory effect in polymer laminates. *Mater. Lett.* **2008**, 62 (25), 4088−4090.
6. Mao, Y.; Ding, Z.; Yuan, C.; Ai, S.; Isakov, M.; Wu, J.; Wang, T.; Dunn, M. L.; Qi, H. J. 3D Printed Reversible Shape Changing Components with Stimuli Responsive Materials. *Sci. Rep.* **2016**, 6, 24761.
7. Peng, Q.; Wei, H.; Qin, Y.; Lin, Z.; Zhao, X.; Xu, F.; Leng, J.; He, X.; Cao, A.; Li, Y. Shape-memory polymer nanocomposites with a 3D conductive network for bidirectional actuation and locomotion application. *Nanoscale* **2016**, 8 (42), 18042−18049.
8. Belmonte, A.; Lama, G. C.; Gentile, G.; Cerruti, P.; Ambrogi, V.; Fernández-Francos, X.; De la Flor, S. Thermally-triggered freestanding shape-memory actuators. *Eur. Polym. J.* **2017**, 97, 241−252.
9. Behl, M.; Kratz, K.; Noechel, U.; Sauter, T.; Lendlein, A. Temperature-Memory Polymer Actuators. *Proc. Natl. Acad. Sci. U. S. A.* **2013**, 110 (31), 12555−12559.
10. Behl, M.; Kratz, K.; Zotzmann, J.; Nöchel, U.; Lendlein, A. Reversible Bidirectional Shape-Memory Polymers. *Adv. Mater.* **2013,** 25 (32), 4466-4469.
11. Han, J. L.; Lai, S. M.; Chiu Yu, T. Two-way multi-shape memory properties of peroxide crosslinked ethylene vinyl-acetate copolymer (EVA)/polycaprolactone (PCL) blends. *Polym. Adv. Technol.* **2018**, DOI: 10.1002/pat.4309.
12. Wang, K.; Jia, Y.-G.; Zhu, X. X. Two-Way Reversible Shape Memory Polymers Made of Cross-Linked Cocrystallizable Random Copolymers with Tunable Actuation Temperatures. *Macromolecules* **2017**, 50 (21), 8570−8579.
13. Biswas, A.; Aswal, V. K.; Sastry, P. U.; Rana, D.; Maiti, P. Reversible Bidirectional Shape Memory Effect in Polyurethanes through Molecular Flipping. *Macromolecules* **2016**, 49 (13), 4889− 4897.
14. Bothe, M.; Pretsch, T. Bidirectional Actuation of a Thermoplastic Polyurethane Elastomer. *J. Mater. Chem. A* **2013**, 1 (46), 14491−14497.
15. Gao, Y.; Liu, W.; Zhu, S. Polyolefin Thermoplastics for Multiple Shape and Reversible Shape Memory. *ACS Appl. Mater. Interfaces* **2017**, 9 (5), 4882−4889.
16. Lu, L.; Li, G. One-Way Multishape-Memory Effect and Tunable Two-Way Shape Memory Effect of Ionomer Poly(ethylene-comethacrylic acid). *ACS Appl. Mater. Interfaces* **2016**, 8 (23), 14812−14823.
17. Saatchi, M.; Behl, M.; Nöchel, U.; Lendlein, A. Copolymer Networks From Oligo (ε - caprolactone) and n - Butyl Acrylate Enable a Reversible Bidirectional Shape - Memory Effect at Human Body Temperature. *Macromol. Rapid Commun.* **2015,** 36 (10), 880-884.

18. Zhou, J.; Turner, S. A.; Brosnan, S. M.; Li, Q.; Carrillo, J.-M. Y.; Nykypanchuk, D.; Gang, O.; Ashby, V. S.; Dobrynin, A. V.; Sheiko, S. S. Shapeshifting: Reversible Shape Memory in Semicrystalline Elastomers. *Macromolecules* **2014,** 47 (5), 1768-1776.
19. Farhan, M.; Rudolph, T.; Nöchel, U.; Yan, W.; Kratz, K.; Lendlein, A. Noncontinuously Responding Polymeric Actuators. *ACS Appl. Mater. Interfaces* **2017,** 9 (39), 33559-33564.
20. Xie, T.; Li, J.; Zhao, Q. Hidden Thermoreversible Actuation Behavior of Nafion and Its Morphological Origin. *Macromolecules* **2014**, 47 (3), 1085−1089.
21. Feng, Y.; Behl, M.; Kelch, S.; Lendlein, A. Biodegradable Multiblock Copolymers Based on Oligodepsipeptides with Shape- Memory Properties. *Macromol. Biosci.* **2009**, 9 (1), 45−54.
22. Dai, X.; Zhang, Y.; Gao, L.; Bai, T.; Wang, W.; Cui, Y.; Liu, W. A Mechanically Strong, Highly Stable, Thermoplastic, and Self-Healable Supramolecular Polymer Hydrogel. *Adv. Mater.* **2015,** 27 (23), 3566-71.
23. Feng, Y.; Guo, J. Biodegradable Polydepsipeptides. *Int. J. Mol. Sci.* **2009,** 10 (2), 589-615.
24. Zhang, C.; Hu, J.; Li, X.; Wu, Y.; Han, J. Hydrogen-Bonding Interactions in Hard Segments of Shape Memory Polyurethane: Toluene Diisocyanates and 1,6-Hexamethylene Diisocyanate. A Theoretical and Comparative Study. *J. Phys. Chem. A* **2014,** 118 (51), 12241-12255.
25. Feng, Y.; Lu, J.; Behl, M.; Lendlein, A. Progress in Depsipeptide‐Based Biomaterials. *Macromol. Biosci.* **2010,** 10 (9), 1008-1021.
26. Crescenzi, V.; Manzini, G.; Calzolari, G.; Borri, C. Thermodynamics of fusion of poly-β-propiolactone and poly-ϵ-caprolactone. comparative analysis of the melting of aliphatic polylactone and polyester chains. *Eur. Polym. J.* **1972,** 8 (3), 449-463.
27. Fernandez‐d'Arlas, B.; Corcuera, M.; Runt, J.; Eceiza, A. Block architecture influence on the structure and mechanical performance of drawn polyurethane elastomers. *Polym. Inter.* **2014,** 63 (7), 1278-1287.
28. Qi, H.; Boyce, M. Stress–strain behavior of thermoplastic polyurethanes. *Mech. Mater.* **2005,** 37 (8), 817-839.
29. Yan, W.; Fang, L.; Weigel, T.; Behl, M.; Kratz, K.; Lendlein, A. The Influence of Thermal Treatment on the Morphology in Differently Prepared Films of a Oligodepsipeptide Based Multiblock Copolymer. *Polym. Adv. Technol.* **2016,** 28 (10), 1339-1345.
30. May‐Hernandez, L.; Hernandez‐Sanchez, F.; Gomez‐Ribelles, J.; Serra, S. i. Segmented poly (urethane‐urea) elastomers based on polycaprolactone: Structure and properties. *J. Appl. Polym. Sci.* **2011,** 119 (4), 2093-2104.
31. Seymour, R.; Estes, G.; Cooper, S. L. Infrared studies of segmented polyurethan elastomers. I. Hydrogen bonding. *Macromolecules* **1970,** 3 (5), 579-583.
32. He, Y.; Xie, D.; Zhang, X. The structure, microphase-separated morphology, and property of polyurethanes and polyureas. *J. Mater. Sci.* **2014,** 49 (21), 7339-7352.
33. Byler, D. M.; Susi, H. Examination of the secondary structure of proteins by deconvolved FTIR spectra. *Biopolymers* **1986,** 25 (3), 469-487.
34. Huang, M.; Zheng, L.; Wang, L.; Dong, X.; Gao, X.; Li, C.; Wang, D. Double Crystalline Multiblock Copolymers with Controlling Microstructure for High Shape Memory Fixity and Recovery. *ACS Appl. Mater. Interfaces* **2017,** 9 (35), 30046-30055.
35. Zhu, P.; Dong, X.; Wang, D. Strain-Induced Crystallization of Segmented Copolymers: Deviation from the Classic Deformation Mechanism. *Macromolecules* **2017,** 50 (10), 3911-3921.

36. Matsumiya, Y.; Watanabe, H.; Takano, A.; Takahashi, Y. Uniaxial Extensional Behavior of (SIS)p-Type Multiblock Copolymer Systems: Structural Origin of High Extensibility. *Macromolecules* **2013,** 46 (7), 2681-2695.
37. Yang, H.; Liu, D.; Ju, J.; Li, J.; Wang, Z.; Yan, G.; Ji, Y.; Zhang, W.; Sun, G.; Li, L. Chain Deformation on the Formation of Shish Nuclei under Extension Flow: An in Situ SANS and SAXS Study. *Macromolecules* **2016,** 49 (23), 9080-9088.
38. Wang, L.; Wang, J.-H.; Yang, B.; Wang, Y.; Zhang, Q.-P.; Yang, M.-B.; Feng, J.-M. A novel hierarchical crystalline structure of injection-molded bars of linear polymer: co-existence of bending and normal shish–kebab structure. *Colloid and Polymer Science* **2013,** 291 (6), 1503-1511.
39. Nitta, K.-h. On the Orientation-Induced Crystallization of Polymers. *Polymers* **2016,** 8 (6), 229.
40. Zhao, Y.; Keroack, D.; Prud'homme, R. Crystallization under Strain and Resultant Orientation of Poly(ε-caprolactone) in Miscible Blends. *Macromolecules* **1999,** 32 (4), 1218-1225.